Brazilian Journal of Chemical Engineering (2021) 38:361–372
https://doi.org/10.1007/s43153-021-00104-7

ORIGINAL PAPER

Gas holdup and bubble flow transition characteristics in column flotation process determined by capacitive signals measurement

Sri Harjanto[1] · Didied Haryono[1,2] · Harisma Nugraha[1] · Ginanjar Saputra[2] · Marlin R. Baidillah[3] · Mahfudz Al Huda[3] · Warsito P. Taruno[3]

Received: 12 August 2020 / Revised: 19 December 2020 / Accepted: 15 April 2021 / Published online: 28 April 2021

Abstract

A non-invasive and non-intrusive monitoring techniques are developed based on the signal capacitance method to observe column flotation performance. In general, gas holdup and bubble flow characteristics are the essential parameters that affect flotation performance. This study investigates and verifies the effects of frother dosage and solid percent on the gas holdup and bubble flow transition characteristic by analyzing the capacitance signals. Experiments were conducted in two- and three-phase systems with a variation of frother addition and solid concentration in the range of 1–5 cm/s of superficial gas velocities. The results showed that the capacitance signals method could characterize the bubble flow and its transition in column flotation, which consists of discrete bubbly, cap-discrete bubbly, and slug flow. The bubble flow transition in the three-phase system occurred at slightly lower superficial gas velocity and gas holdup than in the two-phase system, as measured by the deviation of gas holdup analysis. Higher frother addition and the higher solid concentration will decrease the gas holdup of bubble flow transition. In this study, the flow transition occurred between the superficial gas velocity of 2.5–3.3 cm/s for 2 phase and 2.5–3 cm/s for 3 phase systems.

Keywords Capacitance method · Column flotation · Flow characteristic · Gas holdup

List of symbols

ϕ_g	Gas holdup
ε_m	Permittivity of aerated medium
ε_g	Permittivity of gas phase
ε_b	Permittivity of non-aerated medium (liquid phase)
J_g	Superficial gas velocity
C	Measured capacitance
Q	Total charge
$\nabla\Phi$	Potential distribution
ΔV	Voltage difference
H_0	Height of non-aerated medium
ΔH	Height difference of aerated and non-aerated media

Introduction

Column flotation, which was first invented in 1962, is the physicochemical process of a three-phase system (solid, liquid, and gas), that separates valuable mineral from gangue by controlling the hydrophobicity of the minerals particles surface. Since then, its basic understanding and applications had proliferated in the 1980s (Finch and Dobby 1991). The bubbles are generated from the bottom part of the column by injecting the gas into the solid–liquid mixture. Hydrophobic mineral particles, either valuable minerals or gangue, will collide, attach to the bubble due to collector reagents addition in the slurry, and float to the surface of the slurry. In contrast, hydrophilic particles will collide with the bubble without attachment and sink at the bottom of the column. In some industries, column flotation may be utilized in combination with the mechanical flotation process. The column flotation is mainly attributed as a cleaning section, which increases the recovery and grade of a concentrate (Uribe-Salas et al. 2007).

As in general flotation techniques, the column's dispersion properties determine the flotation performance since they relate with the mechanism of particle attachment by the

✉ Sri Harjanto
sri.harjanto@ui.ac.id

1 Department of Metallurgical and Materials Engineering, Universitas Indonesia, Depok 16424, Indonesia

2 Department of Metallurgical Engineering, Universitas Sultan Ageng Tirtayasa, Cilegon 42435, Indonesia

3 Center for Non-Destructive Testing and Process Imaging, CTECH Labs Edwar Technology, Serpong 15235, Indonesia

bubbles (Sanwani et al. 2006). The opportunities for process improvements, therefore, can be provided by studying them (Yianatos et al. 2010).

In the 2 phase and 3 phase system, not only limited in the flotation process, many studies have extensively investigated the dispersion properties by several techniques, such as visual (Chen et al. 2001; Grau and Heiskanen 2003; Matiolo et al. 2011; Nesset et al. 2006; Schwarz and Alexander 2006), electrical or resistance (Banisi et al. 1995a, b; Dahlke et al. 2005; Gomez et al. 2003; Lee et al. 2003; Sanwani et al. 2006; Tavera et al. 2001; Tavera and Escudero 2002), pressure (Hernandez et al. 2003; Shukla et al. 2010), radiation (Yianatos et al. 2010) and resistance or conductance tomography (Nissinen et al. 2014; Vadlakonda and Mangadoddy 2017) techniques. The visual method is mainly used for bubble estimation and flow identification. Electrical, pressure, and phase separation techniques are used for phase holdup analysis. Also, tomography techniques are employed to analyze phase holdups and their distribution because of the capability to provide images. Most studies have reported that optimum flotation performance can be achieved if the flow has a bubbly flow pattern. Since the turbulence is minimal in bubbly flow conditions, the particle-bubbles aggregates are preserved and float successfully. Generally, the bubble flow is set to obtain optimum flotation performance. Therefore, the transition area of the bubbly flow to slug or churn-turbulent flow must be known to achieve the highest recovery and grade of concentrate.

The gas holdup (ϕ_g) is one of the dispersion properties that significantly affects the flotation performance (Connor et al. 1990; Gomez et al. 1991; Sanwani et al. 2006; Tavera et al. 2001; Zhou and Egiebor 1993). The gas holdup is influenced by some variables of chemicals (such as collectors, frothers, activators, and regulators), operational (e.g., airflow, feed rate, wash water), and mechanical aspects (such as cell design and configuration). ϕ_g also defines the bubble-flow density, which corresponds to the flotation kinetics (Gorain et al, 1997). Hence, some attempts have been made to better understand flotation performance by ϕ_g measurements and predictions. Zhou and Egiebor (1993) developed a model to predict the axial ϕ_g profiles of gas and compared their model to other studies. Finch et al. (2000) proposed gas-holdup measurement to replace the bubble surface area flux (Sb)as a machine factor due to its practicability and ease of measurement. Shukla et al. (2010) found that the bubble size increased, and ϕ_g decreased due to bubble coalescence in the presence of particles. Xu et al. (1992) investigated to measure the radial profile of ϕ_g and found that the profile changed from W-shape to saddle-shape as superficial gas velocity increased with three spargers. Saddle-shaped patterns occurred at low superficial gas velocity with one central sparger, and the profile was axisymmetric with one off-center sparger.

In the gas holdup study using electrical techniques, the capacitance technique is another prospective method besides conductance and electrical resistance techniques due to its capability to measure non-invasively and non-intrusively. This technique measures gas holdup (ϕ_g) based on different permittivities of the aerated and non-aerated media, since permittivity is a volumetric function of the dispersed phase. As in the conductance technique, Maxwell's equation may also be used to estimate gas holdup (Gomez et al. 2003).

In this study, bubble flows in the column flotation process are characterized using a capacitive measurement method by analyzing ϕ_g from capacitance signal. Frother dosage and solid concentration (wt%) are the main parameters used in this study. This study aims to investigate those effects on ϕ_g and its characteristic as well as the bubble flow transition. A high-speed camera is used for confirming the flow and analyzing the bubble size.

Gas holdup measurement by capacitance method

Φ_g measurement using the capacitance technique is derived by solving the Laplace equation (Geraets and Borst 1988). Some models have been developed in particular applications for determining ϕ_g accurately. In the case of the flotation process, Maxwell's model given by Eq. (1) has been used extensively (Gomez et al. 2003) because this model considers small spheres that disperse uniformly in a continuous phase (liquid or slurry). In the capacitance technique, the conductivity effect is kept as low as possible for minimizing error in ϕ_g measurement using Maxwell's model. Therefore, demineralized water is used in this study to reduce the effect of conductivity (see Table 1). For comparison in estimating ϕ_g, models of series, parallel, and complex refractive index (CRI) given by Eqs. (2), (3), and (4), respectively, are also included (Jaworek and Krupa 2010).

$$\phi_g = \frac{1 - \left(\frac{\varepsilon_m - \varepsilon_g}{\varepsilon_b - \varepsilon_g}\right)}{1 + 0.5\left(\frac{\varepsilon_m - \varepsilon_g}{\varepsilon_b - \varepsilon_g}\right)} \quad (1)$$

Table 1 The relative permittivity and conductivity of materials used in this study

Material	Relative permittivity (ε_r)	Conductivity (S/m) (σ)
Air (for 0.9 MHz)	1.0006	–
Demineralized water (at 25 °C)	78.5	$<2\times10^3$
SiO_2	4.5	5×10^{-14}

$$\phi_g = \left[\left(\frac{\varepsilon_b \cdot \varepsilon_g}{\varepsilon_b - \varepsilon_g} \right) \cdot \frac{1}{\varepsilon_m} \right] - \frac{\varepsilon_g}{\varepsilon_b - \varepsilon_g} \quad (2)$$

$$\phi_g = \left(\frac{1}{\varepsilon_g - \varepsilon_b} \right) \cdot \varepsilon_m - \frac{\varepsilon_b}{\varepsilon_g - \varepsilon_b} \quad (3)$$

$$\phi_g = \left(\frac{\sqrt{\varepsilon_m} - \sqrt{\varepsilon_b}}{\sqrt{\varepsilon_g} - \sqrt{\varepsilon_b}} \right) \quad (4)$$

ϕ_g (-) is the gas holdup; ε_m (-), ε_g (-), and ε_b (-) are the permittivities of the aerated medium, air (100%), and non-aerated medium, respectively.

For the calibration of the capacitance technique, the lowest and highest permittivity materials are considered, which consist of air (ε_g) and non-aerated medium (ε_b), demineralized water mixed with a small amount of frother less than 40 ppm (40 mg/L). Since specific information about the electrical permittivity of frother used in this study is not available, the calibration of the highest permittivity is conducted by mixing demineralized water with a frother to overcome the permittivity change caused by frother concentration. The relative permittivity (ε_r) of air, demineralized water, and SiO_2 is shown in Table 1 (Drake et al. 1930; Schön 2011).

In the case of a three-dimensional medium, the general relationship of measured capacitance and permittivity is given as Eq. (5).

$$C = \frac{Q}{\Delta V} = -\frac{1}{\Delta V} \oiint_s \varepsilon(x, y, z) \nabla \phi(x, y, z) dS \quad (5)$$

Here, C is the measured capacitance, Q is the total charge as a function of permittivity (ε), and $\nabla\phi$ is the potential distribution (or electric field). ΔV is the voltage difference between the electrodes, and S is the area enclosing the receiver electrode. The measured capacitance increases with increasing relative permittivity because $C \propto \varepsilon$. In this case, since the relative permittivity of air is lower than the demineralized water, the rise in ϕ_g decreases the measured capacitance. Therefore, by knowing the permittivity as measured capacitance, ϕ_g can be estimated using those models in Eqs. (1)–(4).

Materials and methods

Materials

In this simulated laboratory scale flotation study, demineralized water as the liquid phase was used with the addition of DowFroth ® 1012 as the frother agent. As the solid phase, SiO_2, which has a purity of 99% and a particle size distribution in the range of 105–149 micron, was utilized. The pure SiO_2 was used to minimize the conductivity effect and increase the accuracy of gas holdup measurement.

Capacitance sensor design

The capacitance sensor mainly consists of electrodes that act as the transmitter and receiver electrodes, as well as a guard electrode. Transmitter and receiver electrodes have a function to excite and receive the signal corresponding to measured capacitance. The guard/ground electrode acts to maximize the uniformity of the electric field distribution radially and axially by reducing the edge effects (non-linear electric fields) (Abouelwafa et al. 1980). Thus, the electric fields received by the receiver electrode are uniform since the non-linear response of the capacitance sensor will cause an error of ϕ_g measurement (Ahmed 2006). Therefore, the capacitance sensor design is crucial for accurately measuring ϕ_g because the difference in the geometry of electrodes affects the distribution of the electric field inside the volume of measurement, consequently affecting the sensitivity and response of the sensors (Ahmed 2006). In this study, the concave-type capacitance sensor (Fig. 1), a modification of previous studies (Ahmed 2006; Hewitt and Hall-Taylor 1970), has the highest sensitivity for measuring ϕ_g among all capacitance design sensors.

A customized data acquisition system (DAS; C-Tech Labs Edwar Technology; model: DAQ013202, 2016) was used in this study. The DAS has a signal excitation of 18.4 Vpp (sine wave) and a working frequency of 2.5 MHz, and the acquisition rate was up to 200 frames per second (fps) for one pair of the electrode. The signal to noise ratio (SNR) of this system was 52 dB for measuring demineralized water object, which has a variance 2 times smaller than when measuring demineralized water with superficial gas velocity 1 cm/s. It indicates that the fluctuation comes from the behavior inside the column, not the noise of equipment.

Experimental procedure

Experiments were conducted in a simulated condition of laboratory-scale column flotation cell having an internal diameter of 4.6 cm and a height of 125 cm. Filter disc or sparger used has 16–40 µm pore sizes (P3; Duran). The capacitance measurement system and a personal computer were connected to the flotation column. The capacitance sensor was attached to the outer column surface at the center of the collection zone (Fig. 2). As shown in the dashed line box of Fig. 2, only one electrode pair was used in this study. The high-speed camera was installed at 75 cm from the bottom column, above the capacitance sensor for visualizing the hydrodynamics conditions and comparing ϕ_g measurements.

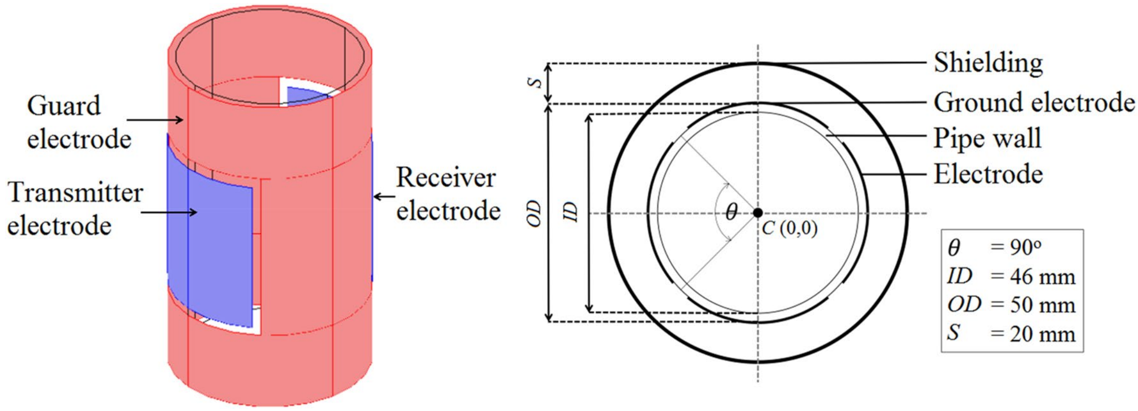

Fig. 1 Schematic of a concave-type two-electrode capacitance sensor design

Fig. 2 Schematic arrangement of laboratory-scale column flotation equipped with a capacitance measurement device

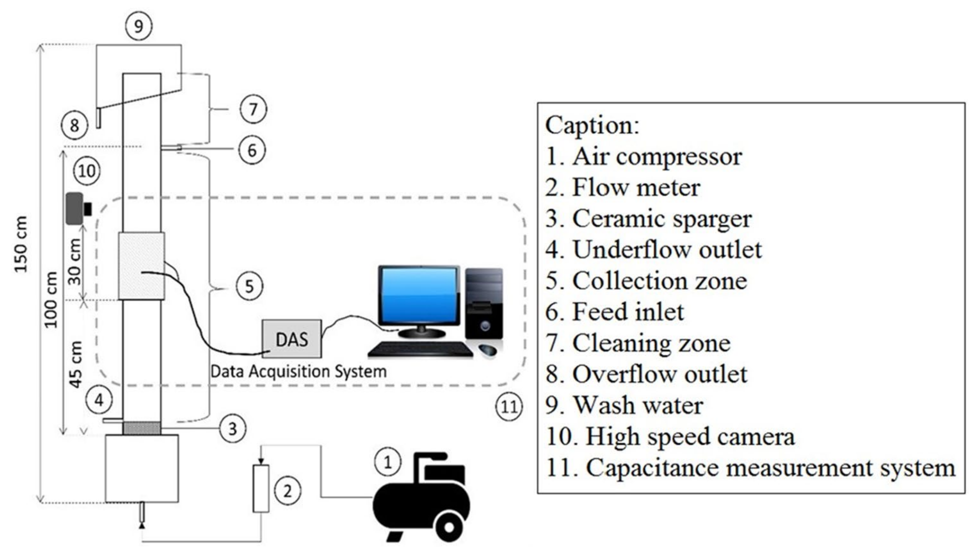

Also, bubble images from the camera were used to estimate the bubble size using image analysis software. The bubble's size was measured from a modified pipe (flat surface) to eliminate bias due to the curved tube. Sauter diameter (D_{32}) was then calculated and compared with those measured by drift flux analysis.

In the three-phase system, frother (DowFroth® 1012) was added to the 500 cm^3 demineralized water and conditioned for up to 5 min. First, the bubbles were generated, and wash water was operated, then the solid particles (SiO_2) was fed into the column. Air bubbles were produced by injecting normal air from the bottom of the column using a compressor, while wash water was pumped from above of the column using a pump. The capacitance signals were captured for 30 s of each variable with the frother dosage addition was 10 and 20 ppm. The solid concentration used in this experiment was 1, 5, and 10 wt%. Each variable was injected by air at the superficial gas velocity from 2 to 4 cm/s. Statistical analysis using three-ways ANOVA and multi regression analysis were conducted to interpret the gas holdup data from the measurements (Jackson 2009; Venkateshan 2015).

To estimate the gas holdup (ϕ_g), derived from Eqs. (1)–(4), accurately, an alternative method using the height difference measurement of the aerated and non-aerated media was performed for standardization. ϕ_g estimation by using height difference measurement was given by Eq. (6) where H_0 is the height of the non-aerated medium, ΔH is the height difference of aerated and non-aerated media. ϕ_g estimation from the height difference measurement of aerated and non-aerated media was used as a standard. Therefore, the model closest to the standard would be used for further data analysis.

$$\phi_g = \frac{\Delta H}{\Delta H + H_0} \tag{6}$$

Results and discussion

Gas holdup models evaluation

Figure 3 shows the comparison ofgas holdup obtained from the models ($\phi_{g\text{-m}}$) given by Eqs. (1)–(4) and the gas-holdup obtained from the height of difference measurements ($\phi_{g\text{-}std}$). It shows that the preferred model of the study is the Maxwell and CRI models since the models' curves are closest to the diagonal line (measurement curve). The parallel and series models show overestimated and underestimated the gas holdup (ϕ_g), respectively. The relative deviation (RE) is used to evaluate these models' accuracy (see Eq. 7), where $\phi_{g\text{-}m}$ and $\phi_{g\text{-}std}$ are the gas holdup value from models and from the height difference measurements, respectively.

$$\text{RE} = \left| \frac{\phi_{g-m} - \phi_{g-std}}{\phi_{g-std}} \right| x100\% \tag{7}$$

As shown in Table 2, the series and parallel models show high relative errors, which are 48% and 22%, respectively. On the other hand, both Maxwell and CRI models show the same relative errors, which are 8%. Therefore, either the Maxwell or CRI model can be used for further data analysis. In this study, the Maxwell model is used for the data analysis since it is more common in the flotation study.

Table 2 Relative error comparison in estimating the gas holdup of each model using the capacitance signals measurement

Model	Relative error (%)
Maxwell	8
Series	48
Parallel	22
CRI	8

Bubble size analysis

Figure 4 shows a relation between sauter mean diameter (D_{32}) and superficial gas velocity at different frother concentration. Black-square, black-triangle, and black-circle lines indicate D_{32} with the frother concentration of 0 ppm (no frother), 10 ppm, and 20 ppm, respectively. While the dashed lines indicate D_{32} for 10 and 20 ppm frother estimated using drift-flux analysis (Dobby et al. 1988). The trend of D_{32} measured from the camera and the drift-flux analysis have relatively similar patterns. As shown in Fig. 4, D_{32} only changes slightly as superficial gas velocity increases, especially for 10 and 20 ppm frothers. However, the distribution of D_{32} tends to increase as the superficial gas velocity increases. It is indicated by the deviation of D_{32}, in which it increases from the superficial gas velocity of 3 cm/s. The increase of superficial gas velocity (more than 4 cm/s) tends to change the flow pattern from bubbly to slug flow, which turbulency in the bubble flow becomes significant. Therefore, bubble sizes become more heterogeneous. Thus, it makes the deviation tend larger. However, at the same superficial gas velocity, D_{32} decreases as frother concentration increases, particularly for lower superficial gas velocity (1–2.5 cm/s). D_{32} of this study has a similar result with the previous study (Grau et al. 2005), D_{32} obtained for DowFroth ® 1012 is about 2.2 mm with critical coalescence concentration (CCC) at 6.6 ppm, and D_{32} above CCC still decreases slightly. It means that this result agrees well with the study of Grau et al. (2005).

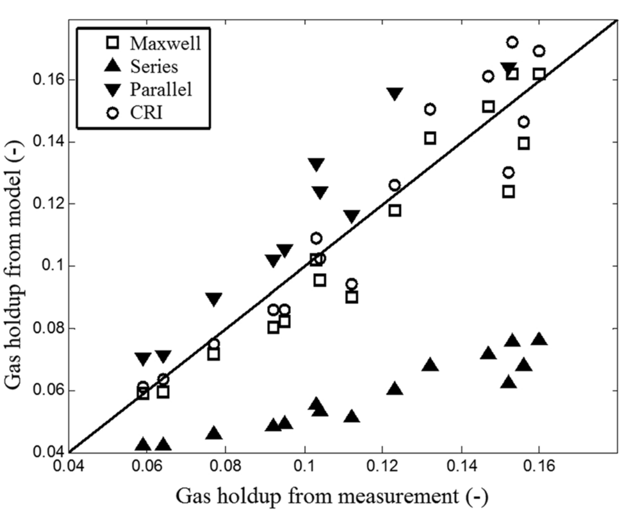

Fig. 3 Comparison of gas holdup estimated from models given by Eqs. (1)–(4) and the height measurements in a laboratory-scale column flotation experiment

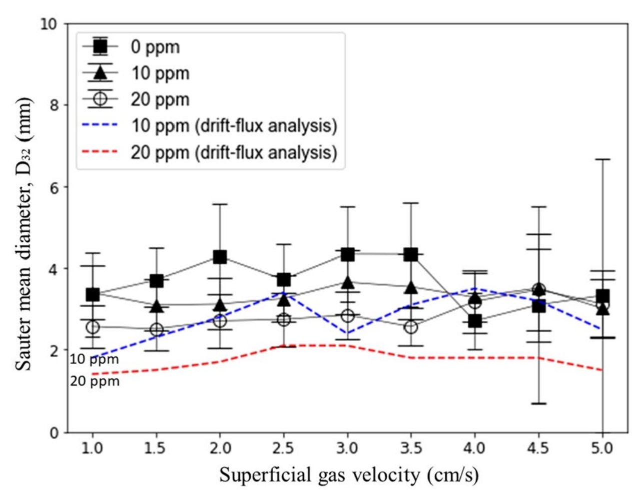

Fig. 4 Relation of D_{32}, drift-flux analysis and superficial gas velocity at different frother concentration in two-phase system

Flow visualization and gas holdup characteristics

Figure 5 shows flow visualizations of two- and three-phase systems captured using a high-speed camera at 75 cm from the bottom of the column representing different flow patterns. These images were obtained from the dosage of 20 ppm at superficial gas velocities of 2, 3, and 4 cm/s for both two- and three-phase systems showing bubbly (Fig. 5a, d), cap-bubbly (Fig. 5b, e), and slug flow (Fig. 5c, f), respectively. As shown in Fig. 5, the bubbly flow pattern is indicated by the relatively similar bubble size. The cap-bubbly flow pattern is observed appearing in the center of the column. The slug flow pattern is indicated by the large bubble having a size close to the column's diameter. In the three-phase system (Fig. 5d, e and f), the interpretation of the flow pattern's images was interfered with by solid particles. Additional lines around the bubbles were made to show the morphology of the bubbles in the column. It is still difficult to compare the bubble size between 2 and 3 phase system from the high-speed camera images (Fig. 5d, e and f). Theoretically, in the 3 phase system with the same condition of frother addition and superficial gas velocity of 2 phase system, the bubble size is relatively larger due to coalescence induced by solid particles in the slurry resulting in larger bubbles that have higher rise velocity.

Figure 6 shows the gas holdup (ϕ_g) characteristics of two-phase (Fig. 6a–e) and three-phase (Fig. 6f–j) column flotation process as functions of time and frother dosage. Gas holdup (ϕ_g) characteristics of two-phase and three-phase at a particular time were characterized by using capacitive signals for 30 min measurements in different superficial gas velocities, i.e., 2.0, 2.5, 3.0, 3.5, and 4 cm/s.

Generally, at low superficial gas velocity (J_g), the bubbles are generated individually from the sparger and do not interact with each other (or weak interaction), resulting in a dispersed phase. In contrast, at high Jg, individual bubbles are triggered to collide with each other and form cap-bubbles. At a particular condition, a slug flow pattern may develop when the bubble size diameter grows close to the column diameter. Based on hydrodynamic conditions within the column, there are three types of bubble flow patterns, namely, discrete bubbly, cap-discrete bubbly, and slug flow patterns. A detailed explanation of the flow pattern and its transition can be obtained in the previous study (Hewitt and Hall-Taylor 1970).

The capacitance signals measurement shown in Fig. 6a–j may represent the hydrodynamic conditions within the column, such as discrete bubbly, cap-discrete bubbly, and slug flow patterns as depicted by the high-speed camera observation. Comparison of ϕ_g measurement using capacitance technique and visual inspections by using high-speed

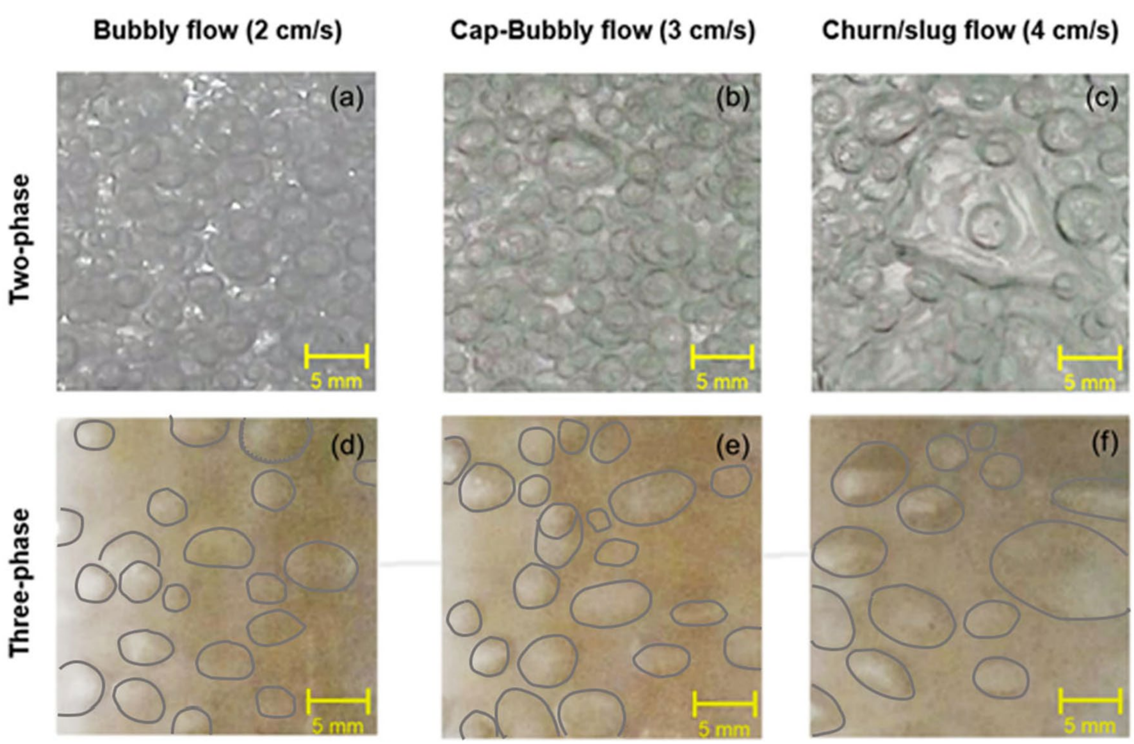

Fig. 5 Bubble flow visualizations using a high-speed camera of two-phase (**a**, **b**, **c**) and three-phase (**d**, **e**, **f**) systems with the dosage of 20 ppm frother at superficial gas velocities of 2 cm/s (**a**, **d**), 3 cm/s (**b**, **e**) and 4 cm/s (**c**, **f**)

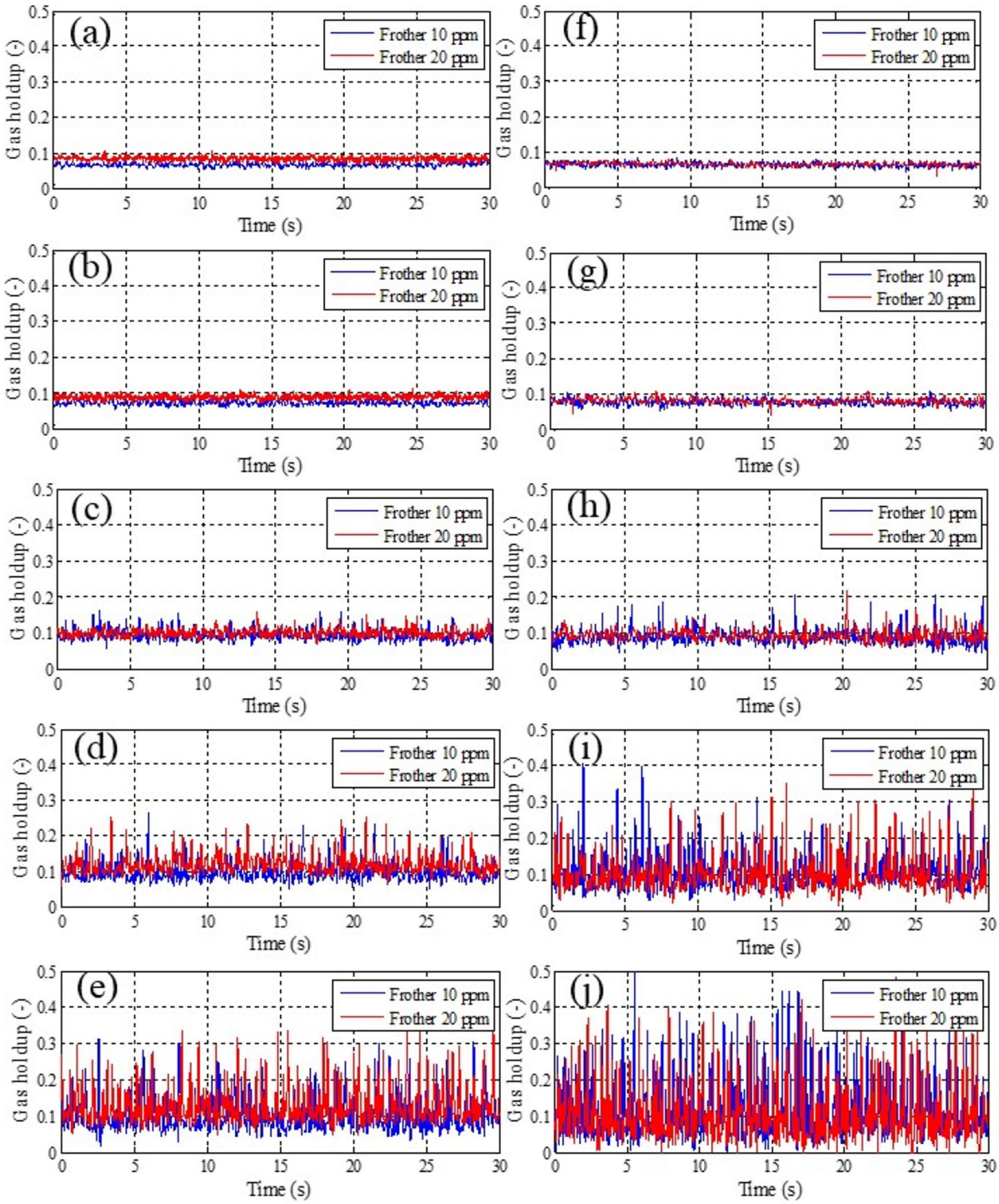

Fig. 6 Gas holdup in the two-phase (**a**–**e**) and three-phase (**f**–**j**) column flotation processes obtained by the capacitance signals measurement, 2 cm/s (**a**, **f**), 2.5 cm/s (**b**, **g**), 3 cm/s (**c**, **h**), 3.5 cm/s (**d**, **i**), and 4 cm/s (**e**, **j**). (Color figure online)

camera confirms the discrete bubbly flow at the superficial gas velocity of 2.0 and 2.5 cm/s both in two- and three-phase systems (Fig. 6a, b, f and g). The slug flow pattern in the column of two-phase can be observed using the high-speed camera at the higher superficial gas velocity of 4 cm/s, indicated by a large bubble close to the diameter of the column. On the contrary, it is difficult to observe the slug flow pattern in 3 phase system using high-speed camera due to its turbidity. In general, it is challenging to observe the transition flow pattern or cap discrete bubbly flow visually using a high-speed camera since most of them appear on the center of the column covered by the bridge of dispersed bubbles.

Actually, by observing the ϕ_g signal patterns of two- and three-phase systems (Fig. 6), the bubble flow patterns can be distinguished between discrete bubbly and slug flow. Even, it is difficult to determine the transition flow pattern or cap-discrete flow. Besides, the effect of higher frother addition to the increase of ϕ_g signals can be observed in the two-phase system at low superficial gas velocity. The difference between their surface tensions causes the difference between the peak frequencies of ϕg signals for 10- and 20-ppm frother dosages. It is because the surface tension relates to the bubbles generated inside the column. Surface tension governs bubble size and its distribution. Lower surface tension will produce smaller bubbles. The effect of surface tension on the characteristics of the bubbles can be explained by the Weber number (Pistorius 2013). The Weber number explains the relation between the inertia to the surface tension forces, in which the higher the Weber number, the larger the bubble size. And also, the higher Weber number tends to produce non-spherical bubble. Inertia force is affected by the bubble rise velocity, while the surface tension force is affected by the frother addition. In this case, the difference of Weber number is caused by the change of frother dosage, which changes the column's bubble characteristics. Therefore, it will impact the measurement of ϕg signals. The 20-ppm frother dosage has a lower surface tension, resulting in a smaller cap-bubble within the column. Otherwise, it is difficult to be observed the effect of frother addition to the ϕ_g signals in 3 phase system. With this condition for the two-phase system, the cap-discrete bubbly flow pattern can be predicted to appear at J_g of 3 cm/s. When J_g is increased beyond 3 cm/s, the slug flow pattern is obtained, which is caused by the higher intensity of bubble–bubble collisions than in the cap-discrete bubbly flow pattern.

Considering the limitation of ϕ_g signals observations in the two- and three-phase system, further ϕ_g signals analysis is undertaken by calculating the deviation of ϕ_g. The deviation of ϕ_g is calculated by using the standard deviation equation of ϕ_g signals on two- and three-phase systems. Compared with variance values, standard deviation values have more conformity with visual observation using a high-speed camera.

Figure 7 shows an analysis of flow pattern transition using the standard deviation of ϕ_g signal on two- and three-phase systems and bubble flow pattern indication using ϕ_g signals. In Fig. 7a, the deviation of ϕ_g at superficial gas velocity is plotted. There are two areas of plot, i.e., horizontal and slope fields. The deviation of the gas holdup of both two- and three-phase systems in superficial gas velocity less or equal to 2.5 cm/s are similar. In the slope area, the three-phase system has a higher deviation of ϕ_g. The effect of frother concentration addition on the deviation of gas hold up seems not to occur in the two- and three-phase systems. By using the intersection of the regression line in the horizontal and slope area, the transition zone of flow patterns can be determined. In the two- and three-phase systems, the transition of bubble flow may occur in the range of 2.5–3.3 cm/s and 2.5–3.0 cm/s, respectively. The difference in the flow transition between two- and three-phase systems is caused by the solid particles which intensify the collision between bubbles and bubble-particle. ϕ_g below 0.1 indicates

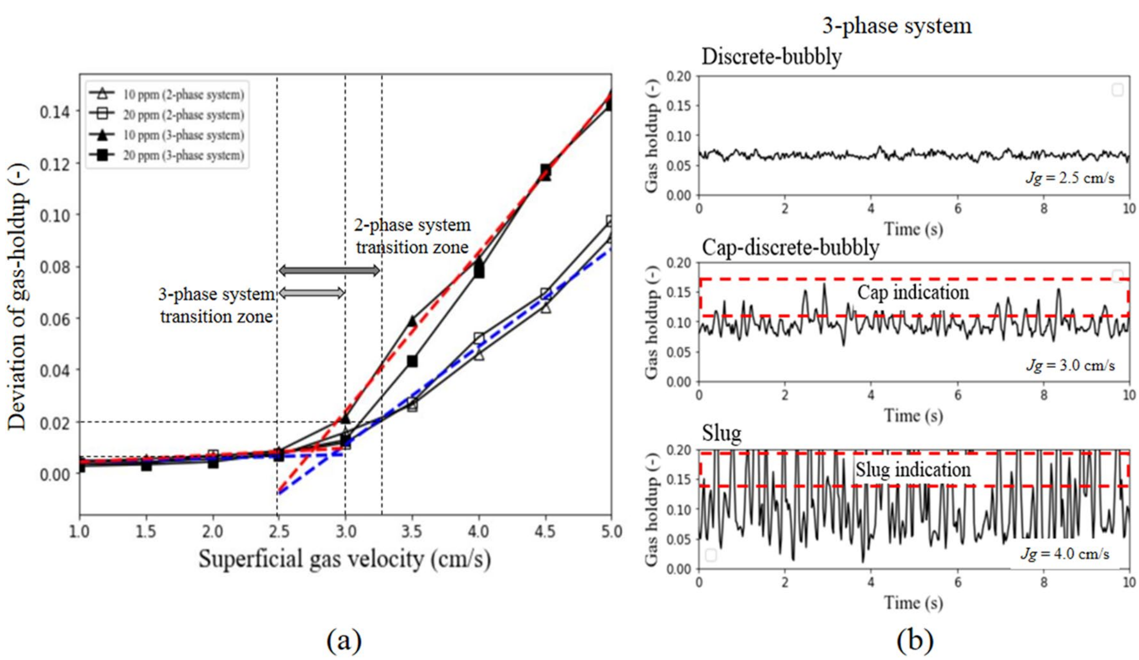

Fig. 7 Flow transition analysis on 2- and 3-phase system using the deviation of gas-holdup (**a**), bubble flow pattern indication by gas holdup signal characteristics in three-phase system (**b**). (Color figure online)

for discrete-bubbly flow pattern, ϕ_g with the peaks ranging from 0.1 to 0.15 indicates cap-discrete-bubbly flow pattern, and ϕ_g with the peaks above 1.5 indicates slug flow pattern (see Fig. 7b).

Relationship of gas holdup and superficial gas velocity

Figure 8 (a) and (b) shows the relationship between ϕ_g and J_g representing the effects of frother dosage (100 ppm and 200 ppm) in two-phase and three-phase system respectively. The bubble flow characteristics were plotted in the Fig. 8 (a) and (b), which was obtained from the projection of capacitance signals deviation into superficial gas velocity illustrated in Fig. 7a. Three areas are representing the bubble flow characteristics: discrete bubbly, cap-discrete bubbly, and slug flow. In the two-phase system, the gas holdup of cap-discrete bubbly (transition of discrete-bubbly and slug flow) occurs at the range of 0.07–0.09 (10 ppm frother) and 0.09–0.11 (20 ppm frother). In the three-phase system, the gas holdup of cap-discrete bubbly occurs in the range of 0.04–0.07 (10 ppm frother) and 0.07–0.08 (20 ppm frother). From this result, the range of the gas holdup of cap-discrete bubbly, which is the transition of discrete-bubbly and slug flow, in the three-phase system are lower than those of the two-phase system.

Detailed data distribution and descriptive statistics of Fig. 8a and b can be seen in Figure S1 and Table S1 in Electronic Supplementary Materials. Based on statistical analysis using three-ways ANOVA (Table S3, Electronic Supplementary Materials), the population of means of phase, frother addition, and superficial gas velocity in Fig. 8a and b are significantly different in the significance level of 0.05. It means that the variables significantly affect the gas holdup, even the standard deviation bars are overlapping (Fig. S1 and Fig. S2). Further statistical analysis using regression analysis (Table S5, column 2 and 3, Electronic Supplementary Materials) shows that the gas holdup increase with increasing superficial gas velocity. Also, higher frother concentration in a certain superficial gas velocity gives higher gas holdup. However, the frother's impact on the increase of the gas holdup is higher when the superficial gas velocity is higher than the lower superficial gas velocity. This condition can be seen from the interaction between gas velocity and frother (in Table S5, columns 2 and 3), which is positive (0.000709 for 2 phase and 0.00104 for 3 phase) and statistically significant at 1% interval.

Higher frother addition, surface tension becomes lower at the interface, reducing the power requirement for creating bubbles (Gomez et al. 1991). Therefore, the bubble size is smaller, resulting in a larger total bubble surface area than the highest surface tension at the interface, which gives higher gas holdup. However, detailed observation in the transition area, cap-discrete bubble flow shows a pulsating gas holdup in the superficial gas velocity of 2 – 3 cm/s, especially for 0 and 10 ppm for 2 phase. The slope ($\Delta\phi_g$ / ΔJ_g) is negative in the range of superficial gas velocity of 2.5–3 cm/s for 0 ppm and 3–3.5 cm/s for 10 ppm frother addition. This phenomenon is not observed in the previous study using electrical resistance probe method (Gomez et al. 1991; Vadlakonda et al. 2017). Since the slope ($\Delta\phi_g$ / ΔJ_g) also indicates the rise velocity of the bubble swarm (Finch et al. 2007), pulsating gas holdup in the certain range of superficial gas velocity reflects pulsating rise velocity of bubble swarm. Lower rise bubble swarm velocity gives higher gas hold up, whereas higher rise bubble

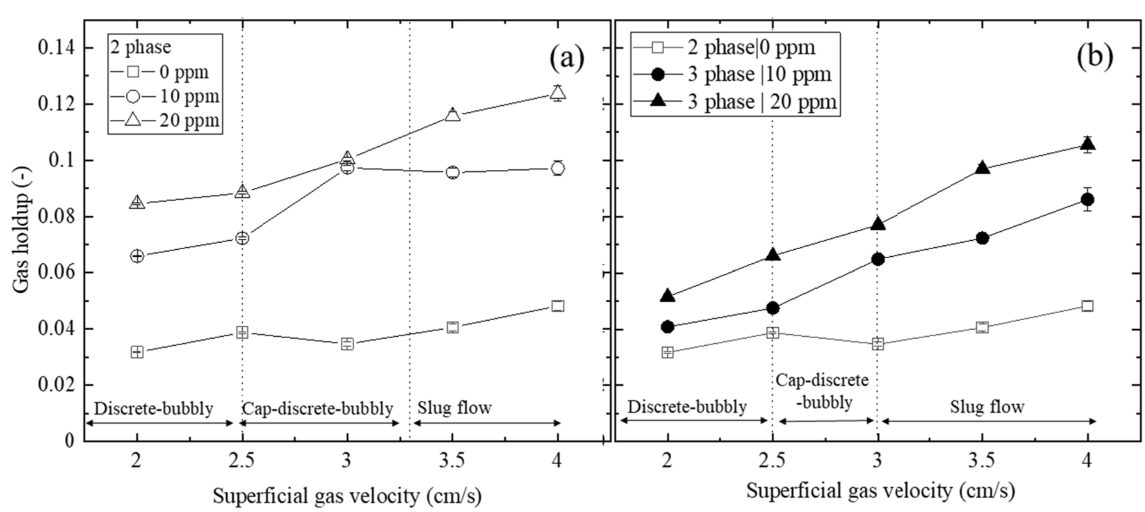

Fig. 8 Effect of superficial gas velocity on gas holdup with a variation of frother concentration in flotation column and bubble flow transition characteristics for 2-phase (**a**) and 3 phase (**b**), at 10 wt% solid concentration. Standard errors of means bars are included in the graphs. Some bars are not shown in the graph due to their small values

swarm velocity reduces gas holdup. This phenomenon is not observed for the higher frother addition (20 ppm) or lower surface tension in the 3 phase system.

Figure 9 illustrates the effect of superficial gas velocity with a variation of solid concentration in the 3 phase system of 10 ppm and 20 ppm frother addition. Detailed data distribution and descriptive statistics of Fig. 9 can be seen in Fig. S2 and Table S2 in Electronic supplementary Materials. By using three-ways ANOVA, the population means of gas holdup from variations of superficial gas, solid-weight percentage, and frother addition and their combination are significantly different at 0.05 significance level. Further analysis using regression show that in average, the higher solid weight percentage decreases gas holdup. Simultaneously, the effect of frother addition to the gas holdup decreases as the superficial gas velocity increases.

As shown in Fig. 9a and b, the increase of solid concentration decreases the gas holdup at the same superficial gas velocity. The common difficulty in explaining the effect of solid weight percentage to the gas holdup in column flotation is the limited observation of the bubbles' morphology due to its turbidity. However, Banisi, et al. (1995a, b) explained this phenomenon by the two mechanisms, i.e. (1) change in radial gas holdup distribution and (2) bubble wake effects. The first mechanism is that the solid concentration within the column will affect the liquid–gas circulation due to the column's solid dispersion. The change of liquid–gas circulation will physically impact the bubble terminal rise velocity, thus to its radial gas holdup distribution. In which, at the presence of the solid, the radial gas holdup becomes non-uniform. This evidence has been validated using the drift flux model analysis. The second mechanism relates to the role of viscosity. In which the presence of solid within the column will increase the viscosity of the slurry. In this condition, the bubble wake tends to shift from unstable to stable when solid particles are added. Therefore, it increases the bubble rise velocity and impacts on the decrease of gas holdup. It is also observed in Fig. 9 (a), (b) that in lower solid concentration(1 wt%), the gas holdup reaches a peak at the superficial gas velocity of 3.5 cm/s in 10 ppm and 20 ppm frother addition. The increasing solid concentration fraction from 5 wt% to10 wt% may decrease the gas holdup by about 30% (in 10 ppm frother addition) and 17% (in 20 ppm frother addition). In the 3 phase system, decreasing gas holdup with increasing the solid concentration becomes lower at higher superficial gas velocity (more than 3.5 cm/s).

In general, the trend shown in Figs. 8 and 9 agrees with the previous study (for instance, Mena et al. 2008). However, it should be noted that this study used SiO_2 as solid particles in the laboratory scale of the flotation column process in a three-phase system. The observation of the bubble and solid particle interaction is limited to bubble flow and its interaction with solid particles in the slurry without considering the effect of solid particle attachment on the bubble surface because no collector reagent was added in this study. Accordingly, at this stage of the study, the flotation performance in terms of concentrate recovery could not be calculated. Therefore, a further detailed study on the capacitance signal method measurement for column flotation monitoring by using ore samples is still underway.

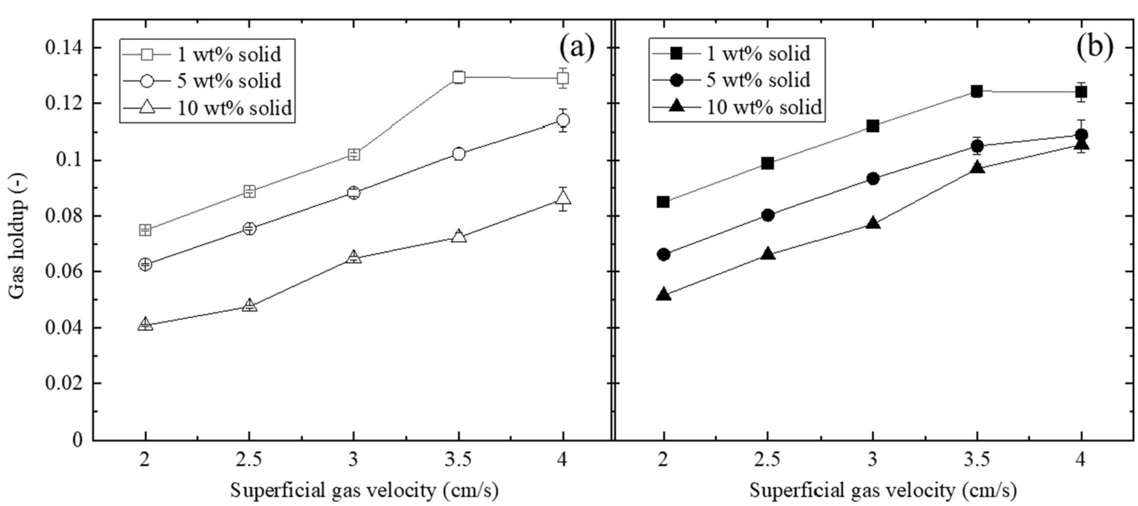

Fig. 9 Effect of superficial gas velocity on gas holdup in the three-phase system of the flotation column with a solid concentration variation in 10 ppm frother addition (**a**) and 20 ppm frother addition (**b**). Standard errors of means are included in the graphs. Some are not shown in the graph due to their small values

Conclusions

Bubble flow characteristics in column flotation were characterized by gas holdup measurement using the capacitance technique in a laboratory column flotation cell, which was derived by using Maxwell's model. The results showed that the capacitance method successfully characterized the bubble flow in laboratory-scale column flotation, consisting of discrete bubbly, cap-discrete bubbly, and slug flow patterns, as confirmed with visual observation. Their transition flow characteristics were also successfully determined quantitatively by standard deviation analysis of capacitance signals. The flow transition zone or cap-discrete bubbly zone occurred at the superficial gas velocity ranging from 2.5 to 3.0 cm/s for 3 phase system and 2.5–3.3 for 2 phase system. The transition zone of the three-phase system, i.e., cap-discrete bubbly flow, had lower superficial gas velocity than that of the two-phase system. The addition of higher frother (from 10 to 20 ppm) concentration decreases the gas holdup in the superficial gas velocity range. The gas holdup also decreases in higher solid weight concentration. Higher frother addition in the 3 phase system of column flotation reduce the gas holdup at a certain superficial gas velocity and solid weight concentration.

Supplementary Information The online version contains supplementary material available at https://doi.org/10.1007/s43153-021-00104-7.

Acknowledgements Authors acknowledge Research Grant of the Primary Research of Higher Education scheme from Directorate of Research and Community Engagement Ministry of Research, Technology and Higher Education of the Republic of Indonesia 2018–2019. The authors express their gratitude to Dr. Muhammad H. Yudhistiro of Universitas Indonesia to discuss statistical analysis.

References

Abouelwafa MSA, Kendall EJM (1980) The use of capacitance sensors for phase multiphase pipelines. IEEE Trans Instrum Meas 29:24–27

Ahmed WH (2006) Capacitance sensors for void-fraction measurements and flow-pattern identification in air – oil two-phase flow. IEEE Sens J 6:1153–1163

Banisi S, Finch JA, Laplante AR, Weber ME (1995a) Effect of solid particles on gas holdup in flotation columns-II. Investigation of mechanisms of gas holdup reduction in presence of solids. Chem Eng Sci 50:2335–2342

Banisi S, Finch JA, Laplante AR, Weber ME (1995b) Effect of solid particles on gas holdup in flotation columns - I. Measur Chem Eng Sci 50:2329–2334

Chen F, Gomez CO, Finch JA (2001) Bubble size measurement in flotation machines. Miner Eng 14:427–432

Connor CTO, Randall EW, Goodall CM (1990) Measurement of the effects of physical and chemical variables on bubble size. Int J Miner Process 28:139–149

Dahlke R, Gomez C, Finch JA (2005) Operating range of a flotation cell determined from gas holdup vs. gas rate. Miner Eng 18:977–980

Dobby GS, Yianatos JB, Finch JA (1988) Estimation of bubble diameter in flotation columns from drift flux analysis. Can Metall Q 27:85–90

Drake FH, Pierce GW, Dow MT (1930) Measurement of the dielectric constant and index of refraction of water and aqueous solutions of KCl at high frequencies. Phys Rev 35:613–622

Finch JA, Dobby GS (1991) Column flotation: a selected review. Part I Int J Miner Process 33:343–354

Finch JA, Xiao J, Hardie C, Gomez CO (2000) Gas dispersion properties: bubble surface area flux and gas holdup. Miner Eng 13:365–372

Finch JA, Cilliers J, Yianatos J (2007) Column flotation. In: Froth flotation in century of innovation, eds.: M. C. Fuerstenau, G. Jameson and R-H. Yoon, Society of Mining, Metallurgy and Exploration, 681–708

Geraets JJM, Borst JC (1988) A capacitance sensor for two-phase void fraction measurement and flow pattern identification. Int J Multiph Flow 14:305–320

Gomez CO, Uribe-Salas A, Finch JA, Huls BJ (1991) Gas hold-up measurement in flotation columns using electrical conductivity. Can J Metall Mater Sci 30:201–205. https://doi.org/10.1179/cmq.1991.30.4.201

Gomez CO, Cortes-Lopez F, Finch JA (2003) Industrial testing of a gas holdup sensor for flotation systems. Miner Eng 16:493–501

Gorain BK, Franzidis JP, Manlapig EV (1997) Studies on impeller type, impeller speed and air flow rate in an industrial scale flotation cell. Part 4: effect of bubble surface area flux on flotation performance. Miner Eng 10:367–379

Grau RA, Heiskanen K (2003) Gas dispersion measurements in a flotation cell. Miner Eng 16:1081–1089

Grau RA, Laskowski JS, Heiskanen K (2005) Effect of frothers on bubble size. Int J Miner Process 76:225–233

Hernández H, Gómez CO, Finch JA (2003) Gas dispersion and de-inking in a flotation column. Miner Eng 16:739–744

Hewitt GF, Hall-Taylor NS (1970) Annular Two-Phase Flow. Pergamon Press, pp 50–74

Jackson SL (2009) Research methods and statistics-a critical thinking approach, Wadsworth, pp 290–315

Jaworek A, Krupa A (2010) Phase-shift detection for capacitance sensor measuring void fraction in two-phase flow. Sens Actuators A 160:78–86

Lee J-E, Choi W-S, Lee J-K (2003) A study of the bubble properties in the column flotation system. Korean J Chem Eng 20(5):942–949

Matiolo E, Testa F, Yianatos J, Rubio J (2011) On the gas dispersion measurements in the collection zone of flotation columns. Int J Miner Process 99:78–83

Mena PC, Rocha FA, Teixeira JA, Sechet P, Cartellier A (2008) Measurement of gas phase characteristics using a monofibre optical probe in a three-phase flow. Chem Eng Sci 63:4100–4115

Miller RS (1985) Photographic observations of bubble formation in flashing nozzle flow. J Heat Transfer 107:750

Nesset JE, Hernandez-aguilar JR, Acuna C, Gomez CO, Finch JA (2006) Some gas dispersion characteristics of mechanical flotation machines. Miner Eng 19:807–815

Nissinen A, Lehikoinen A, Mononen M, Lähteenmäki S, Vauhkonen M (2014) Estimation of the bubble size and bubble loading in a flotation froth using electrical resistance tomography. Miner Eng 69:1–12

Pistorius PC (2013) Bubbles in process metallurgy. In: Treatise on process metallurgy, vol. 2. Elsevier Ltd, pp 179–196

Sanwani E, Zhu Y, Franzidis JP, Manlapig EV, Wu J (2006) Comparison of gas holdup distribution measurement in a flotation cell using capturing and conductivity techniques. Miner Eng 19:1362–1372. https://doi.org/10.1016/j.mineng.2006.01.006

Schön J (2011) Physical properties of rocks: a workbook. Elsevier, Oxford, p 276

Schwarz S, Alexander D (2006) Gas dispersion measurements in industrial flotation cells. Miner Eng 19:554–560

Shukla SC, Kundu G, Mukherjee D (2010) Study of gas holdup and pressure characteristics in a column flotation cell using coal. Miner Eng 23:636–642

Tavera FJ, Escudero R (2002) Gas holdup and solids holdup in flotation columns: on-line measurement based on electrical conductivity. Miner Process Extr Metall 111:94–99. https://doi.org/10.1179/mpm.2002.111.2.94

Tavera FJ, Escudero R, Finch JA (2001) Gas holdup in flotation columns : laboratory measurements. Int J Miner Process 61:23–40

Uribe-Salas A, Pérez-Garibay R, Nava-Alonso F (2007) Operating parameters that affect the carrying capacity of column flotation of a zinc sulfide mineral. Miner Eng 20:710–715. https://doi.org/10.1016/j.mineng.2007.01.008

Vadlakonda B, Mangadoddy N (2017) Hydrodynamic study of two phase flow of column flotation using electrical resistance tomography and pressure probe techniques. Sep Purif Technol 184:168–187. https://doi.org/10.1016/j.seppur.2017.04.029

Venkateshan SP (2015) Mechanical measurement 2nd ed., John Wiley and Son Ltd., West Sussex, 47–70

Xu M, Finch JA, Huls BJ (1992) Measurement of radial gas holdup profiles in a flotation column. Int J Miner Process 36:229–244

Yianatos J, Contreras F, Díaz F (2010) Gas holdup and RTD measurement in an industrial flotation cell. Miner Eng 23:125–130. https://doi.org/10.1016/j.mineng.2009.11.003

Zhou ZA, Egiebor NO (1993) Technical note prediction of axial gas holdup profiles in flotation column. Miner Eng 6:307–312